SAE Paper 97203

INVESTIGATION OF OIL TRANSPORT MECHANISMS ON THE PISTON SECOND LAND OF A SINGLE CYLINDER DIESEL ENGINE, USING TWO-DIMENSIONAL-LASER-INDUCED FLUORESCENCE

Benoist Thirouard, Douglas P. Hart.

Sloan Automotive Laboratory
Massachusetts Institute of Technology
Cambridge, MA, U.S.A.

ABSTRACT

A two-dimensional-Laser-Induced-Fluorescence (LIF) system was developed to visualize the oil distribution and study the oil transport in the piston ring pack of a single-cylinder diesel engine through an optical window on the liner. The system gives high spatial and intensity resolutions so that detailed oil distribution on the piston as well as between the rings and the liner can be studied. This work primarily focused on investigating different oil transport mechanisms on piston second land under various engine operating conditions. Two mechanisms for the oil flow on the second land were identified, namely, inertia driven oil flow in the axial direction and oil dragging by gas flow in the circumferential direction. Finally, the effects of ring rotation were investigated.

1. INTRODUCTION

Reduction of oil consumption is required to satisfy three factors that currently govern the development of automotive engines: utilization of hydrocarbon resources, protection of the environment, and customer satisfaction. It is estimated that more than 50% of the engine oil consumption in automotive engines is from the piston ring pack. Consequently, the investigation of oil transport mechanisms at the interface between piston and liner is of critical importance.

The ring and groove geometry along with temperature and pressure conditions at the interface between piston and liner are the governing factors in oil flow. Due to lack of experimental data, the effects of these parameters on oil transport in the piston ring-pack were poorly understood. Thus, accurate prediction of oil consumption is nearly impossible.

LIF technique have been used for measuring oil film thickness of the piston ring-pack for some time [Hoult and Takigushi (1991), Shaw *et al* (1992), Tamai (1995), Casey (1998), Takigushi *et al* (1998)]. In early works, LIF was implemented to make point measurements. A great deal of knowledge on the oil film thickness between rings and the liner and on the piston was gained by using these systems. However, the obvious limitation of point LIF is that it can only display the oil film at one location and is thus not able to simultaneously show the oil distribution in the piston ring-pack. When one intends to study oil transport in piston ring-pack, it was often found to be very difficult to interpret the data from these measurements without knowing the oil film in the surrounding region [Casey (1998)].

Inagaki et al. (1995) developed a two-dimensional oil film distribution measuring system, where a flash lamp was used as the light source. Even with a narrow window, their system demonstrated the benefits of having a two-dimensional view of oil distribution on a piston. In the current study, a two-dimensional oil distribution measuring system was developed utilizing a pulsed laser. The system was implemented in a single cylinder diesel engine with a 7mm wide window on the cylinder liner. Studies were conducted at varying engine operating conditions and utilizing different ring configurations. Several important oil transport mechanisms were identified. Theoretical models are presented to describe oil flow due to different driving forces.

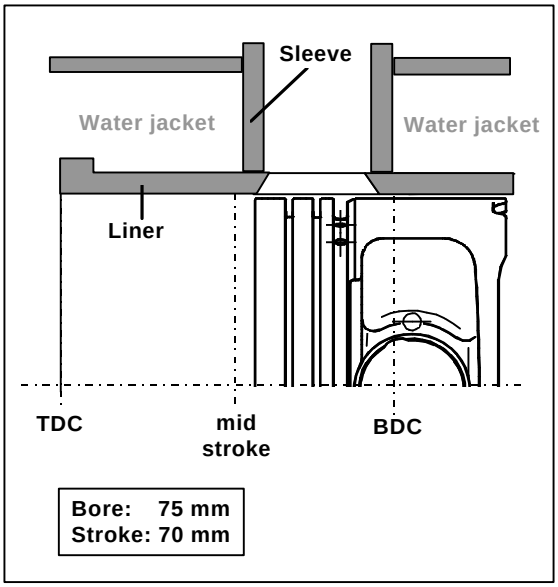

Fig. 1 Engine Setup

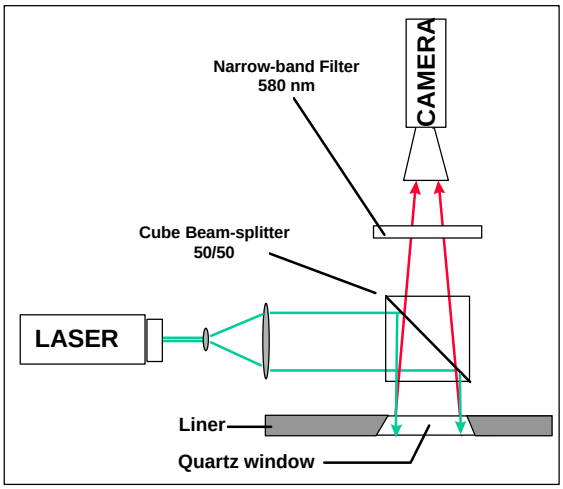

Fig. 2 Optical Setup

2. EXPERIMENT SETUP

2.1 Engine Setup

The engine used in this study was a 300 cc Kubota single-cylinder diesel. The liner was equipped with a quartz window on the anti-thrust side (Fig 1). The window is located between mid-stroke and the BDC so that the entire axial extent of the piston ring-pack can be observed at 88 degree of crank angle before or after the TDC. The window was glued in the liner with Epoxy. Although, the window and the liner were honed together in order to obtain a flush surface, the window was still a few micron protruded after honing. However, ring profiles showed no damage after more than 20 hours running.

2.2 Optical Setup

Laser induced fluorescence was used to observe oil behavior in the piston ring pack. As reported by Röhrle (1995), temperature in the piston ring pack can vary from 80°C on the piston skirt up to 280°C on the crown land. Hence, to resolve all the regions in the piston ring-pack, the sensitivity of the LIF signal to oil temperature must be minimized. The dyes commonly used for this type of experiment are Coumarin 540 and 523 [Hoult and Takigushi (1991), Shaw *et al* (1992), Inagaki *et al* (1995), Takigushi *et al* (1998)]. These dyes, however, are sensitive to temperature. In this work, Rhodamine 590 was chosen for its strong stability with temperature up to 250°C. The implemented dye concentration was 5.10^{-4} mol/liter of oil. The wavelength of maximum absorption for rhodamine 590 is 528 nm. Accordingly, the second harmonic of a Nd YAG laser (532 nm) was used to excite the doped oil. The fluorescence signal was acquired with an intensified CCD camera (Princeton Instrument ICCD 576 SE) through a narrow band filter centered on 580 nm (Fig. 2). The purpose of the narrow band filter was to suppress any effect of direct reflection from the quartz window.

The acquisition frequency was limited by the camera characteristics to 1 frame per second. High spatial resolution was obtained at 0.04 mm/pixel (Fig 3). In the images, the brighter the signal is, the higher the film thickness is. No calibration was attempted in this work. Therefore, observation were qualitative. The system was only able to detect accumulation of the oil in liquid form. As described by Burnett (1992), oil can also be vaporized or be transported as an oil mist in air stream. The current system is not able to detect oil in gaseous and mist forms.

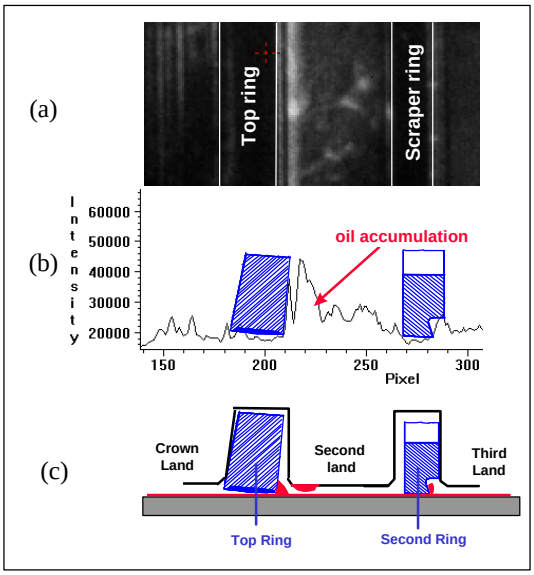

Fig. 3
(a)- Oil distribution image
(b)- Fluorescence intensity across the image
(c)- Ring pack geometry

2.3 Test Specifications

For the experimental results discussed in this paper the engine was equipped with standard rings. Three different ring configurations were tested.

- Configuration 1: top two rings pinned with gaps located on the window side (Fig 4).
- Configuration 2: top two rings pinned with gaps located on the side opposite to the window (Fig 4).
- Configuration 3: standard configuration: non-pinned rings.

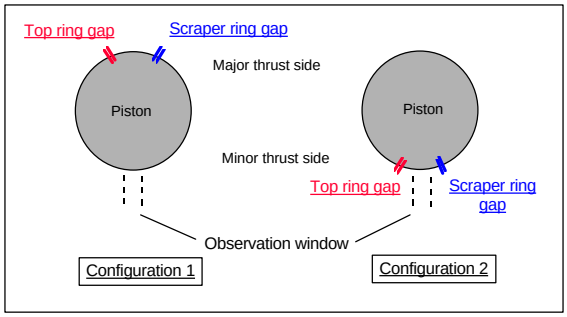

Fig.4 Ring gap location in configurations 1 and 2.

Experiments were conducted from 1200 rpm to 2800 rpm and from no load to 60% load. Coolant temperature was kept constant at 50°C. SAE 10W30 oil was used. Due to the pollution by combustion soot, oil had to be changed every 8 hours.

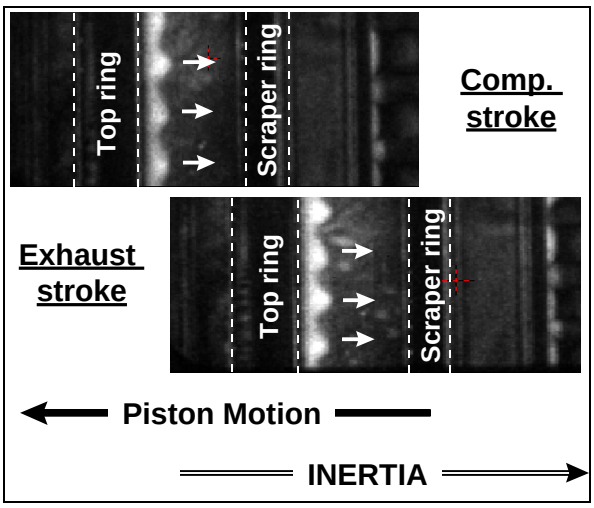

Fig. 5 Inertia driven flow on the second land (1200 rpm - no load - Configuration 3).

3. OIL BEHAVIOR ANALYSIS

Images acquired in configuration 3 during the four strokes of a engine cycle, at 1200 and 1700 rpm, and no load, have shown two important types of oil flows occurring on the piston second land:

1- Oil flow in the cylinder axis direction,
2- Oil flow around the piston circumference.

3.1 Oil Flow in the Axial Direction

Oil flow in the axial direction, driven by the inertia force due to piston acceleration/deceleration was observed. The images shown in Figure 5 were acquired around mid-stroke during the compression and exhaust strokes. The direction of the inertia force switches to the downward direction after the middle of the down-strokes until the middle of the next up-stroke. Since the images are acquired at 88 degree before the TDC for both compression and exhaust

stroke, they should show the maximum effects of downward inertia force on the oil accumulation. As seen in figure 5, the pattern of the oil accumulation below the top ring clearly shows that the oil was moving toward the second ring.

The velocity of oil moving on a flat area under inertia force can be estimated from Tian (1995).

$$V_{oil} = \frac{a.h^2}{u} \qquad \text{(Eq. 1)}$$

where V: Oil velocity.
a : Acceleration .
h : Thickness of the oil accumulation.
ν : Kinematic viscosity.

This equation can be established from a balance of inertia and shear stress, and neglecting the effect of surface tension. The displacement of oil accumulation during the period between a mid down-stroke and mid up-stroke (180 crank angle degrees) was calculated at 1200 rpm for two different oil accumulation thickness:

- h = 10 µm, oil displacement = 0.3 mm
- h = 20 µm, oil displacement = 4 mm.

These results show a very strong effect of oil film thickness on the oil velocity. During the experiments with non-pinned rings (configuration 3), the thickness of the oil on the piston second land was changing continuously so that it was possible to see different oil accumulation patterns at different oil film thickness. As shown in figure 6, with a thicker oil film thickness on the second land (bottom figure), indicated by a strong fluorescence signal, oil motion could be identified from the oil pattern. In the top figure where a thinner oil film thickness exists, no oil flow in the axial direction was observed.

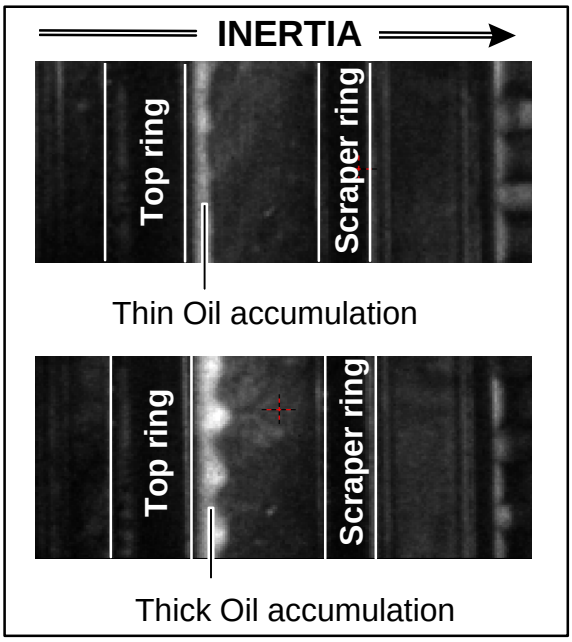

Fig. 6 Inertia driven flow on the second land (1200 rpm - no load - Configuration 3).

One characteristics of the inertia driven oil flow is that the net displacement of the oil in the axial direction over an engine cycle is not significant, as inertia switches direction after every half engine revolution. Unless the film thickness is large enough so that inertia can drive the oil out of the second land, oil would always move back and forth on the second land.

3.2 Oil Transport in the Axial Direction

Strong oil motion around the piston circumference was observed on the second land. The images shown in figure 7 were acquired 10 engine cycles apart. A clear 3 mm/s circumferential flow can be identified on the second land.

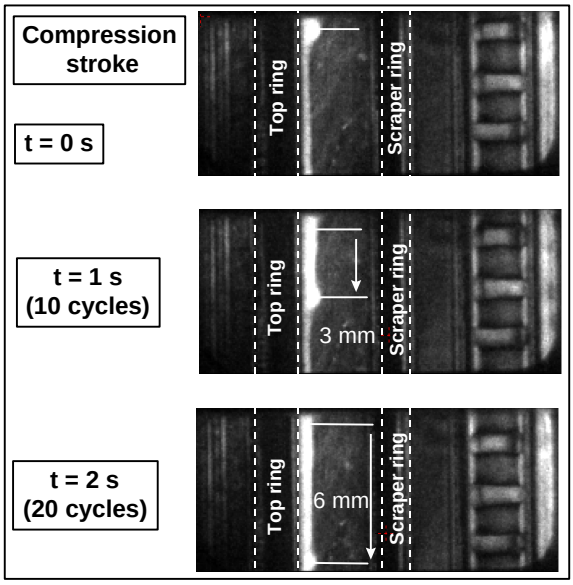

Fig. 7 Oil transport on the second land in the circumferential direction.
(1200 rpm - no load - Configuration 3)

The oil flow in the circumferential direction can be driven by the gas flow. When the cylinder pressure is high, there is a gas flow on the second land from the top ring gap to the second ring gap. The shear stress at the interface of gas and oil drags the oil along with gas. Here, estimation is made to relate the velocity of the oil flow to the gas flow by balancing the shear stress at the gas-oil interface. Because the clearance between the second land and the liner is of the order of 0.2 mm and the axial width of the second land is of the order of 3mm, the gas flow in the circumferential direction can be approximated as uniform across the axial extent of the second land. Thus, the Reynolds number of the gas flow in the channel between the second land the liner can be estimated as:

$$\mathrm{Re} = \frac{\dot{V}\, r}{Lm}$$

where $\dot{V}$: Volumetric flow rate.
ρ : Gas density.
μ : Gas viscosity.
L : Axial width of the second land.

Using the blow-by value of this engine as the estimation of the volumetric flow rate $\dot{V}$, we found that the Reynolds number is below 1000. Consequently, the gas flow in the second land is laminar. Approximating the gas flow in the second land as a Poiseuille flow and the oil flow as a Couette flow, balancing the shear stress at the gas/oil interface gives the following relationship:

-shear stress balance: $\frac{dP}{dx} \cdot \frac{h_{gas}}{2} = m \cdot \frac{V_{oil}}{h_{oil}}$ (Eq. 2)

where
P : Pressure.
V_{oil} : Oil velocity at the gas/oil interface.
h_{gas} : Thickness of the gas layer between the piston and the liner.
h_{oil} : Thickness of the oil layer on the second land.

$$\dot{V} = \frac{L}{12 \cdot m} \cdot \frac{dP}{dx} \cdot h_{gas}^3 \qquad \text{(Eq. 3)}$$

- Combining Eq. 2 and 3, we obtained:

$$V_{oil} = \frac{6 \cdot \dot{V} \cdot h_{oil}}{L \cdot h_{gas}^2}$$

Assuming an oil film thickness of 40 μm, the calculated oil velocity is about 2 mm/s. This result is of the same order of magnitude as the observed velocity. Consequently, it can be concluded that the gas dragging effect is the main force driving oil in the circumferential direction.

There are two characteristics of this oil flow dragged by the gas flow:

- After one engine cycle, positive blow-by implies that there is more gas flow from the top ring gap to the second ring gap than the other way around despite a reversed gas flow starts at around 50 degree after the TDC of the expansion stroke. Thus, the mean oil transport due to the gas dragging effect is directed toward the third land.

- When gas flows down through the top ring gap during the later part of the compression stroke and early part of the expansion stroke, the pressure difference between the combustion chamber and second land pressure is high (Fig. 8). Consequently, the downward gas flow through the top ring gap is usually choked. Thus, the gas velocity in the second land and oil velocity moving by gas dragging is constant with engine speed. The results shown in Figure 8 have been computed using MIT models developed by Tian (1996).

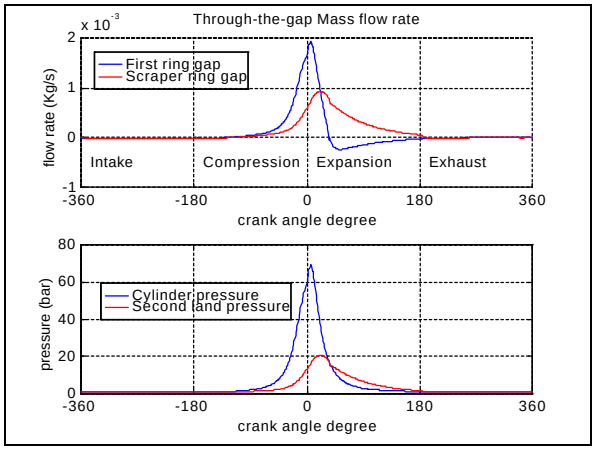

Fig. 8 Mass gas flow through the top two ring gaps and pressure difference at the top ring gap. (1200 rpm - no load).

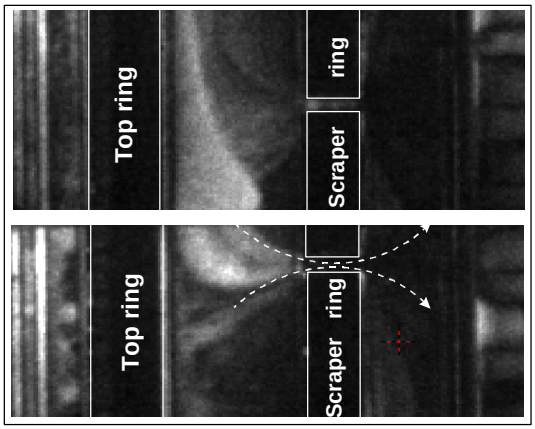

Fig 9 - Oil flow through the scraper ring gap (1200 rpm - no load - compression stroke - Configuration 3).

Occasionally, a clear oil flow pattern just above the second ring gap is observed when the second ring gap rotates to the window location. As shown in Figure 9, oil is pulled toward the scraper ring gap by the gas flow during the compression stroke. However, no oil accumulation was detected in the third land just below the second ring gap (Figure 10). The reason is that the high velocity gas flow in the gap is able to break up the oil and create an oil mist. Oil mist can not be observed on the third land due to low dye concentration.

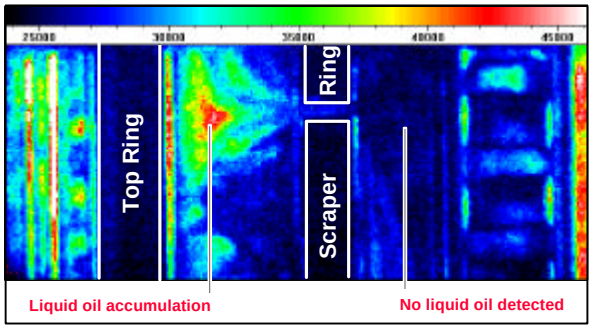

Fig. 10 Oil break up in the scraper ring gap, (1200 rpm - no load - compression stroke - Configuration 3).

3.3 Comparison between Inertia and Gas Dragging Effect

Using the equation proposed to evaluate velocity of oil motion on the second land in the axial direction, the contribution of inertia and gas dragging effects was compared. The following assumptions were made:

- second land width 3 mm,
- oil accumulation lying in the middle of the second land,
- constant blow-by gas velocity on the second land.

If the alternating oil motion induced by inertia is not strong enough for the oil to reach either a ring or a groove, the mean oil axial displacement will be zero. In this case, the gas dragging effect, which continuously drives the oil toward the scraper ring gap, is the main oil transport mechanism on the second land. If inertia can push the oil in one of the two top ring grooves within half an engine revolution,

however, the major flow is in the axial direction and the inertia driven transport becomes the dominant one. In figure 16, a line is drawn to separate two regions where different oil transport mechanisms dominate, based on Eq. 2. In the domain where inertia effect is dominant, oil can be moved across the second land and possibly be transported into the grooves of the top two rings. Part of the oil that flows into the top ring groove then can be transported to the crown land and consumed. In the other domain, the effect of gas dragging is the main mechanism of oil transport in the second land. Effect of the gas dragging eventually removes the oil out of the second land through the ring gaps.

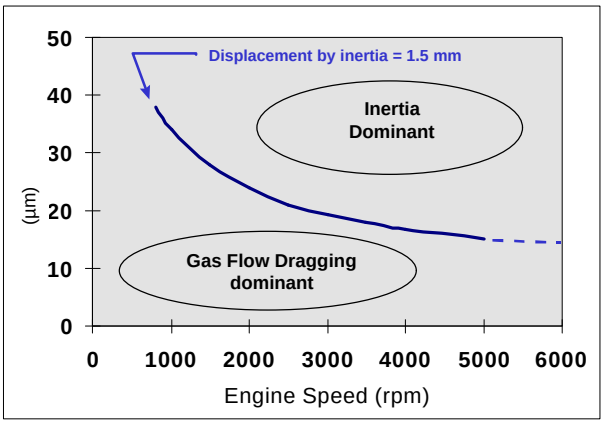

Fig 16 - Comparison of gas dragging and inertia effect on oil transport on the second land.

4. EFFECTS OF RING GAP LOCATION AND RING ROTATION ON SECOND-LAND OIL DISTRIBUTION

4.1 Oil Behavior in Configuration 1

In configuration 1 (Fig. 4), the two top ring gaps were located on the thrust-side, away from the window. In this configuration, strong gas flows do not occur on the second land in front of the observation window. In this case, oil motion on the second land only occurred in the axial direction.

4.2 Oil Behavior in Configuration 2

In configuration 2 (Fig. 4), the top two ring gaps were located on each side of the window, 7 mm away from the window edges. In this configuration, the main gas flow on the second land occurs within the observation window on the anti-thrust side. When the two rings were pinned in configuration 2, no oil accumulation was detected on the piston second land. The strong gas flow which occurs between the two top ring gaps when they are close to each other carries oil into the third land and thus leaves no oil accumulation on the second land at the window location.

4.3 Ring Rotation Effect

In the experiments with non-pinned rings (configuration 3), strong unsteady oil transport was observed. The amount of oil accumulated on the second land changed significantly over several minutes whereas engine parameters were kept constant. In the experiments conducted with the two top rings pinned, however, the oil distribution on the second land was steady. Therefore, it was concluded that ring rotation was responsible for unsteady oil accumulation and oil transport on the second land.

5. CONCLUSIONS

A two-dimensional visualization system using laser-induced-fluorescence was developed to provide detailed images of oil distribution in the piston ring pack of a single cylinder diesel engine. Several mechanisms of liquid oil transport on the piston second land were identified and studied.

Oil was observed moving on the second land in both axial and cicumferential direction.

1- Oil moves in the axial direction when the lubricant accumulation is thick. This was found to be consistent with the fact that inertia driven flows are strongly dependent on oil accumulation thickness.
2- It was observed that the blow-by gas flow drags the oil on the second land in the circumferential direction. This phenomena creates oil accumulation around the second ring gap.

Comparison of both phenomena showed that the gas dragging effect should over take inertia effects at high engine speed.

Finally ring rotation was found to be responsible for unsteady oil behavior on the second land.

AKNOWLEDGMENTS

This work is sponsored by the MIT Consortium on Lubrication in Internal Combustion Engines. Current members include Dana Corporation, Mahle Gmbh, PSA Peugeot Citroën, Renault and Volvo.

REFERENCES

Hoult, D.P., Takigushi, M., 1991, "Calibration of Laser Fluorescence Technique Compared with Quantum Theory," STLE Tribology Transactions, Volume 34 (1991), 3, pp440-444.

Shaw, B.T., Hoult, D.P., Wong, V.W., 1992, "Development of Engine Lubricant Film Thickness Diagnostics Using Fiber Optics and Laser Fluoresence," SAE Paper 920651.

Tamai, G., 1995, "Experimental Study of Engine Oil Film Thickness Dependency on Liner Location, Oil Properties, and Operating Conditions," M.S. Thesis, Department of Mechanical Engineering, MIT.

Casey, S., 1998, "Analysis of Lubricant Film Thickness and Distribution along the Piston/Ring/Liner Interface in a Reciprocating Engine," M.S. Thesis, Department of Mechanical Engineering, MIT.

Takiguchi, M., Nakayama, K., Furuhama, S., Yoshida, H., 1998, "Variation of Piston Ring Oil Film Thickness in an Internal Combustion Engine," SAE Paper 980563.

Inagaki, H., Saito, A., Murakami, M., and Konomi, T., 1995, "Development of Two-Dimensional Oil Film Thickness Distribution Measuring System," SAE Paper 952346.

Röhrle, M.D., 1995, "Pistons for Internal Combustion Engines", MAHLE Gmgh, Printed in Germany 930513.

Burnett, P.J., 1992, "Relationship Between Oil Consumption, Deposit Formation and Piston Motion for Single-Cylinder Diesel Engines," SAE Paper 920089.

Tian, T., Noordzij, B., Wong, V.W., Heywood, J.B., 1996, "Modeling Piston-ring Dynamics, Blow-by, and Ring Twist Effects," ASME ICE Fall Technical Conference, October 1996.

Tian, T., 1995, "Modeling Oil-Transport and Oil-Consumption Mechanisms and the Influence of Piston and Ring Dynamics," Consortium on Lubrication in Internal Combustion Engines, Massachusetts Institute of Technology, June 13 1995, Internal Report.